# Formation of Cage Compounds Containing Boron, Phosphorus, and Transition Metal Atoms

**Tuqiang Chen,[†] Eileen N. Duesler,[†] Robert T. Paine,*[,†] and Heinrich Nöth*[,‡]**

Department of Chemistry, University of New Mexico, Albuquerque, New Mexico 87131, and Institut für Anorganische Chemie, Universität München, 80333 München, Germany

*Received July 31, 1997*

The 1:1 reactions of $(Pr^i_2N)\overline{BP(H)B(N^iPr_2)}PLi\cdot DME$ (**7**) and $(tmp)\overline{BP(H)B(tmp)}PLi\cdot DME$ (**8**) with $(R_3P)_2MCl_2$ (M = Ni, Pd, and Pt) have been surveyed, and bicyclic cage compounds containing boron, phosphorus and transition metal (Ni, Pd, or Pt) atoms have been isolated and characterized. The molecular structures of the species $(Et_3P)_2Pd(PBN^iPr_2)_2$ (**2**), $(Et_3P)_2Pd(PBtmp)_2$ (**3**), and $(Et_3P)_2Pt(PBN^iPr_2)_2$ (**4**) have been determined by single-crystal X-ray diffraction techniques. **2** crystallized in the monoclinic space group *C*2/*c* with $a = 20.212(4)$ Å, $b = 10.225(1)$ Å, $c = 17.460(2)$ Å, $\beta = 107.72(1)°$, and $Z = 4$. **3** crystallized in the orthorhombic space group $P2_12_12_1$ with $a = 12.606(1)$ Å, $b = 12.618(1)$ Å, $c = 24.221(3)$ Å, and $Z = 4$. **4** crystallized in the monoclinic space group *C*2/*c* with $a = 20.195(3)$ Å, $b = 10.187(2)$ Å, $c = 17.280(2)$ Å, $\beta = 107.53(7)°$, and $Z = 4$. The spectroscopic and structural features of the new cage compounds are discussed in relation to their main group element cage analogs.

## Introduction

Recently, two approaches have been established for assembly of cage compounds containing boron and phosphorus atoms.[1−8] One method involves addition of unsaturated carbenoid fragments $ER_n$, e.g., $SnR_2$, to the bicyclic compound $[(tmp)BP]_2$,[2] as illustrated in eq 1. In a similar fashion, zerovalent $(Ph_3P)_2Pt(C_2H_4)$ undergoes oxidative addition to the P−P bond in the $[(tmp)BP]_2$ bicycle producing the cage species $[(tmp)BP]_2Pt(PPh_3)_2$.[2] The use of $(Ph_3P)_4Pd$, however, produces other classes of metalated borylphosphanes.[2] The second method utilizes small boron−phosphorus ring compounds as building blocks and addition and elimination reactions with other main group element moieties to develop the cage structures. This chemistry is shown in general in Scheme 1. Several families of cage compounds, $(R_2NBP)_2ER_n$ ($ER_n$ = $BNR'_2$,[3] $SiR'_2$,[4] $GeR'_2$,[5] $SnR'_2$,[6] and $(SiMe_2)_2$,[4]), $[(R_2NBP)_2]_2Si$,[7] and $[(R_2NBP)_2]_3Si_2$,[8] have now been synthesized in this manner, each in high yield. In this report, further extensions of this chemistry are described which result in the isolation of cage compounds containing boron, phosphorus, and transition metal (Ni, Pd, or Pt) atoms.

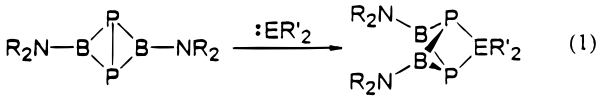


(1)

**Scheme 1**

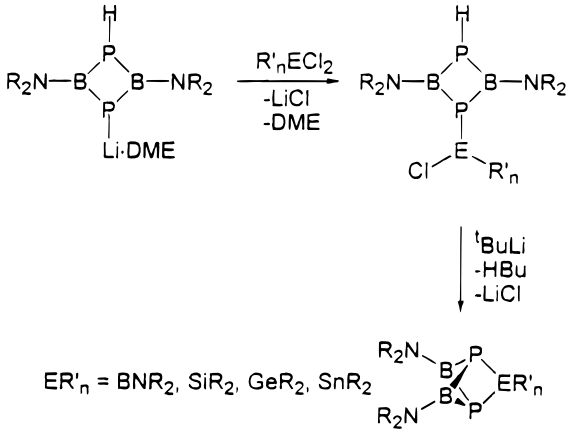


## Experimental Section

**General Information.** Standard inert-atmosphere techniques were used for the manipulation of all reagents and reaction products. Infrared spectra were recorded on a Matteson 2020 FT-IR from KBr pellets. Mass spectra (*m*/*e*) were obtained from the University of Nebraska Midwest Center for Mass Spectrometry by using a Kratos MS-50 spectrometer with FAB analysis. NMR spectra were recorded on Bruker WP-250 and JEOL GSX-400 spectrometers and referenced with $Me_4Si$ ($^1H$, $^{13}C$) and 85% $H_3PO_4$ ($^{31}P$) with $+\delta$ being downfield from the reference. The NMR samples, dissolved in a deuterated lock solvent, were contained in sealed 5 mm tubes.

[†] University of New Mexico.
[‡] Universität München.

(1) Paine, R. T.; Nöth, H. *Chem. Rev.* **1995**, *95*, 343.
(2) Kaufmann, B.; Nöth, H., Schmidt, M.; Paine, R. T. *Chem. Ber.*, submitted for publication.
(3) Dou, D.; Wood, G. L.; Duesler, E. N.; Paine, R. T.; Nöth, H. *Inorg. Chem.* **1992**, *31*, 3756.
(4) Dou, D.; Kaufmann, B.; Duesler, E. N.; Chen, T.; Paine, R. T.; Nöth, H. *Inorg. Chem.* **1993**, *32*, 3056.
(5) Chen, T.; Duesler, E. N.; Paine, R. T.; Nöth, H. *Inorg. Chem.* **1997**, *36*, 802.
(6) Chen, T.; Duesler, E. N.; Paine, R. T.; Nöth, H. *Inorg. Chem.* **1997**, *36*, 1070.
(7) Chen, T.; Duesler, E. N.; Paine, R. T.; Nöth, H. *Phosphorus, Sulfur Silicon*, **1994**, *87*, 41.
(8) Chen, T.; Duesler, E. N.; Paine, R. T.; Nöth, H. *Inorg. Chem.* **1997**, *36*, 1534.

S0020-1669(97)00965-8 CCC: $15.00 
Published on Web 01/16/1998

**Materials.** ($^i$Pr$_2$N)BP(H)B(N$^i$Pr$_2$)PLi·DME[4,9] (**7**) and (tmp)BP(H)B(tmp)PLi·DME[9] (**8**) were prepared as described in the literature. $(Ph_3P)_2PtCl_2$, $(Et_3P)_2PtCl_2$, $(Et_3P)_2PdCl_2$, and $(Et_3P)_2NiCl_2$ were purchased from Aldrich Chemical Co. and used as received. Solvents were rigorously dried and degassed by standard methods. Solvent transfers were accomplished by vacuum distillation, and all reactions and product workups were performed under dry nitrogen.

**Synthesis and Characterization of Compounds. Synthesis.** Compounds **1**−**6** were synthesized in a similar fashion. Typically, equimolar (∼0.5 mmol) amounts of $(R_3P)_2MCl_2$ and **7** or **8** were combined by slow addition of an $Et_2O$ solution (10 mL) of **7** or **8** to a $CH_3CN$ solution (10 mL) of $(R_3P)_2MCl_2$ at 23 °C, and stirred for 16 h. The insoluble materials were filtered off, and crystalline solids were obtained by cooling the filtrates at −10 °C. Compounds **1** (dark brown crystals), **2** and **3** (orange brown crystals), and **4** and **5** (pale yellow crystals) were isolated with yields of 46%, 13%, 30%, 8%, and 19%, respectively. Samples of **6** (orange crystals) were obtained as previously described.[2]

**Characterization. Compound 1.** Mp: 198−200 °C (dec). HRFAB-MS: Calcd for $C_{36}H_{66}{}^{10}B^{11}BN_2P_4{}^{58}Ni$, 657.3786; found, 657.3850; dev, −9.7 ppm. NMR spectra (23 °C, $C_6D_6$): $^{31}P\{^1H\}$, $\delta$ 14.0 ($PEt_3$, pseudo triplet, $^2J_{PP} = 7$ Hz), 6.3 ($P_{cage}$, multiplet, $^2J_{PP} = 7$ Hz); $^1H$, $\delta$ 0.95 m, $CH_3$ in $PEt_3$), 1.64 (m, $CH_2$ in $PEt_3$, overlapped with $CH_2$ groups of tmp), 1.84 ($CH_3$ in tmp); $^{13}C\{^1H\}$, $\delta$ 8.9 (s, $CH_3$ in $PEt_3$), 16.8 (br, $CH_2$ in $PEt_3$), 16.9 (s, tmp), 33.3 (s, tmp), 41.9 (s, tmp), 56.4 (s, tmp). IR ($cm^{-1}$, KBr): 2957 (s), 2935 (s), 2872 (m), 1649 (m), 1633 (m), 1458 (s), 1417 (m), 1389 (s), 1315 (s), 1271 (m), 1234 (w), 1155 (s), 1124 (s), 1035 (s), 912 (w), 771 (m), 707 (w), 561 (w), 507 (w), 470 (w).

**Compound 2.** Mp: 96−100 °C (dec). HRFAB-MS: Calcd for $C_{24}H_{58}{}^{10}B^{11}BN_2P_4{}^{105}Pd$, 624.2824; found, 624.2840; dev, −2.6 ppm. NMR spectra ($C_7D_8$): $^{31}P\{^1H\}$, $\delta$ 12.2 (s, $PEt_3$), −47.3 (s, $P_{cage}$); $^1H$, $\delta$ 0.88−1.01 (m, $CH_3$ in $PEt_3$), 1.26 (d, $CH_3$ in $^i$Pr, $^3J_{HH} = 6.7$ Hz), 1.34 (d, $CH_3$ in $^i$Pr, $^3J_{HH} = 6.7$ Hz), 1.67−1.73 (m, $CH_2$ in $PEt_3$), 3.79 (sept, CH in $^i$Pr, $^3J_{HH} = 6.7$ Hz).

**Compound 3.** Mp: 118−120 °C (dec). HRFAB-MS: Calcd for $C_{30}H_{66}{}^{11}B_2N_2P_4{}^{105}Pd$, 705.3413; found, 705.3451; dev, −5.3 ppm. NMR spectra ($C_6D_6$): $^{31}P\{^1H\}$, $\delta$ 9.9 (m, $PEt_3$, $^2J_{PP} = 6$ Hz), −1.0 (m, $P_{cage}$, $^2J_{PP} = 6$ Hz); $^1H$, $\delta$ 1.84 (s, $CH_3$ in tmp, 24H), 1.71−1.62 (m, $CH_2$ in tmp and in $PEt_3$, 24H), 0.97−0.88 (m, $CH_3$ in $PEt_3$, 18H); $^{13}C\{^1H\}$, $\delta$ 8.7(s, $CH_3$ in $PEt_3$), 16.9 (s, tmp), 17.2 (m, $CH_2$ in $PEt_3$), 33.4 (t, tmp), 42.1 (s, tmp), 56.3 (tmp).

**Compound 4.** Mp: 174−177 °C (dec). HRFAB-MS: Calcd for $C_{24}H_{58}{}^{10}B^{11}BN_2P_4{}^{115}Pt$, 714.34208; found, 714.34246; dev, −0.5 ppm. NMR spectra ($C_6D_6$): $^{31}P\{^1H\}$, $\delta$ 12.1 (d, $PEt_3$, $^1J_{Pt-P} = 3121$ Hz, $^2J_{P-P'} = 19$ Hz), −68.1 (d, $(P-BN^iPr_2)_2$, $^2J_{P-P'} = 18$ Hz); $^1H$, $\delta$ 0.88 (m, 18H, $CH_3$ in Et), 1.30 (d, 12H, $CH_3$ in $^i$Pr, $^3J_{H-H'} = 6.7$ Hz), 1.41 (d, 12H, $CH_3$ in $^i$Pr, $^3J_{H-H'} = 6.7$ Hz), 1.87 (m, 12H, $CH_2$ in Et), 3.86 (sept, 4H, CH in $^i$Pr, $^3J_{H-H'} = 6.7$ Hz); $^{13}C\{^1H\}$, $\delta$ 8.7 (m, $CH_3$ in Et), 19.1 (m, $CH_2$ in Et), 23.6 (s, $CH_3$ in $^i$Pr), 24.0 (s, $CH_3$ in $^i$Pr), 50.1 (s, CH in $^i$Pr). IR (KBr, $cm^{-1}$): 2961 (s), 2928 (s), 2872 (m), 1663 (w), 1626 (m), 1595(m), 1449 (m), 1420 (m), 1362 (m), 1279 (s), 1188 (w), 1146 (m), 1111 (w), 1038 (m), 1009 (w), 777 (m), 717 (m), 634 (w), 435 (w).

**Compound 5.** Mp: 178−180 °C (dec). HRFAB-MS: Calcd for $C_{48}H_{58}{}^{11}B_2N_2P_4{}^{115}Pt$, 1003.33845; found, 1003.342407; dev, −3.9 ppm. NMR spectra ($C_7D_8$): $^{31}P\{^1H\}$, $\delta$ 24.9 (t, $PPh_3$, $^1J_{Pt-P} = 3235$ Hz), −49.5 (s, $(P-BN^iPr_2)_2$); $^1H$, $\delta$ 1.13 (d, 12H, $CH_3$ in $^i$Pr, $^3J_{H-H'} = 6.7$ Hz), 1.31 (d, 12H, $CH_3$ in $^i$Pr, $^3J_{H-H'} = 6.7$ Hz), 3.69 (sept, 4H, CH in $^i$Pr, $^3J_{H-H'} = 6.7$ Hz), 6.89 (Ph), 6.91 (Ph), 7.46−7.52 (Ph); $^{13}C\{^1H\}$, $\delta$ 23.5 (s, $CH_3$ in $^i$Pr), 24.1 (s, $CH_3$ in $^i$Pr), 50.3 (s, CH in $^i$Pr), 127.7 (s, Ph), 134.8 (m, Ph), 137.5 (m, Ph). IR (KBr, $cm^{-1}$): 3051 (m), 2959 (s), 2920 (s), 2862 (m), 1826 (m), 1608 (m), 1589 (m), 1479 (m), 1433 (s), 1360 (m), 1279 (s), 1186 (m), 1143 (m), 1093 (m), 1005 (w), 744 (m), 696 (s), 570 (w), 516 (s), 430 (w).

**Crystallographic Measurements and Structure Solutions.** Single crystals of **2**−**4** were obtained as described above, placed in glass capillaries under a dry nitrogen atmosphere, and sealed. The crystals were centered on a Syntex P3/F automated diffractometer and determinations of crystal class, orientation matrix, and unit cell dimensions were performed in a standard manner. Data were collected in the $\omega$ scan mode with Mo K$\alpha$ ($\lambda = 0.710\,73$ Å) radiation, a scintillation counter, and a pulse height analyzer. Inspection of small data sets led to the assignments of the space groups.[10] Empirical absorption corrections were applied on the basis of $\psi$ scans.[11] Compound **2** showed a small degree of intensity decay (9%), but **3** and **4** displayed no signs of decay.

All calculations were performed on a Siemens SHELXTL PLUS structure determination system.[12] Solutions for the data sets were by heavy atom methods. Full-matrix least-squares refinements were employed,[13] and neutral atom scattering factors and anomalous dispersion terms were used for all non-hydrogen atoms during the refinements. The data collection and refinements for **2** and **4** proceeded in a normal fashion. The heavy atom positions were refined anisotropically, and H atom positions were computed by using the riding model with isotropic $U$'s set at 1.25 $U_{equiv}$ of the parent atom. Compound **3** displayed disorder in the tmp ring containing N(1), which showed a chair conformation (like the tmp ring containing N(2)) as well as a flattened, twisted conformation with equal occupancies. The disordered atoms were not refined anisotropically.

Listings of selected data collection and crystal data are provided in Table 1, and pertinent bond distances and angles are summarized in Table 2. Additional crystallographic data, heavy atom coordinates, H atom coordinates, anisotropic thermal parameters, and full listings of bond lengths and angles are provided in the Supporting Information.

## Results and Discussion

In parallel cage construction studies, Kaufmann et al.[2] observed that the four-vertex bicycle $[(tmp)BP]_2$ undergoes facile P−P bond breaking at 0 °C in the presence of $(Ph_3P)_2Pt(C_2H_4)$ giving the five-vertex bicyclic cage $[(tmp)BP]_2Pt(PPh_3)_2$ (**6**) in high yield (82%). However, a similar 1:1 combination of $[(tmp)BP]_2$ with the zerovalent palladium compound $Pd(PPh_3)_4$ produced a complex product mixture.[2] Two unusual compounds, **9** and **10**, were isolated in low yields, 5% and 13%, respectively, from the mixture. This chemistry is partially represented in Scheme 2. The structure of **9** was proposed on the basis of spectroscopic data, while the structure of **10**, containing a planar $Pd_3P_6$ core, was unambiguously determined by single-crystal X-ray diffraction techniques. There was no evidence for the formation of a five-vertex bicycle $[(tmp)BP]_2Pd(PPh_3)_2$ similar to **6**.[2]

In the present study, an alternative stepwise assembly approach has been employed to form additional examples of the five-vertex cages containing boron, phosphorus, and transition metal (Ni, Pd, or Pt) atoms as summarized in Scheme 3. As shown, the metallaborylphosphane bicyclic cages **1**−**6** are obtained from the 1:1 combination of the lithium phosphide salts **7** and **8** with $(R_3P)_2MCl_2$ (M = Ni, Pd, Pt). The

(9) Dou, D.; Westerhausen, M.; Wood, G. L.; Linti, G.; Duesler, E. N.; Nöth, H.; Paine, R. T. *Chem. Ber.* **1993**, *126*, 379.

(10) Space group notation is given in: *International Tables for X-ray Crystallography*; Reidel: Dordrecht, Holland, 1983; Vol. I, pp 73−346.

(11) The empirical absorption corrections use an ellipsoidal model fitted to azimuthal scan data that are then applied to the intensity data: *SHELXTL Manual*, Revision 4; Nicolet XRD Corp.: Madison, WI, 1983.

(12) Sheldrick, G. M. *Nicolet SHELXTL Operations Manual*; Nicolet XRD Corp.: Cupertino, CA, 1981. SHELXTL uses absorption, anomalous dispersion, and scattering data compiled in: *International Tables for X-ray Crystallography*; Kynoch: Birmingham, England, 1974; Vol. IV, pp 55−60, 99−101, 149−150. Anomalous dispersion terms were included for all atoms with atomic numbers greater than 2.

(13) A general description of the least-squares algebra is found in: *Crystallographic Computing*; Ahmed, F. R., Hall, S. R., Huber, C. P., Eds.; Munksgaard: Copenhagen, 1970; p 187. The least-squares refinement minimizes $\sum w(|F_o| - |F_c|)^2$, where $w = 1/[\sigma(F)_2 + gF_2]$.

**Table 1.** Crystallographic Data for **2**, $(Et_3P)_2Pd(PBN^iPr_2)_2$, **3**, $(Et_3P)_2Pd(PBtmp)_2$, and **4**, $(Et_3P)_2Pt(PBN^iPr_2)_2$

| | **2** | **3** | **4** |
|---|---|---|---|
| chem formula | $C_{24}H_{58}B_2N_2P_4Pd$ | $C_{30}H_{66}B_2N_2P_4Pd$ | $C_{24}H_{58}B_2N_2P_4Pt$ |
| fw | 626.6 | 706.75 | 715.3 |
| cryst syst | monoclinic | orthorhombic | monoclinic |
| space group | *C*2/*c* | $P2_12_12_1$ | *C*2/*c* |
| *a*, Å | 20.212(4) | 12.606(1) | 20.195(3) |
| *b*, Å | 10.225(1) | 12.618(1) | 10.187(2) |
| *c*, Å | 17.460(2) | 24.221(3) | 17.280(2) |
| α, deg | 90 | 90 | 90 |
| *β*, deg | 107.72(1) | 90 | 107.53(7) |
| *γ*, deg | 90 | 90 | 90 |
| *V*, Å$^3$ | 3426.5(9) | 3852.7(6) | 3389.9(9) |
| *Z* | 4 | 4 | 4 |
| $D_{calcd}$, g cm$^{-3}$ | 1.215 | 1.218 | 1.402 |
| *T*, °C | 20 | 20 | 20 |
| *μ*, cm$^{-1}$ | 7.43 | 6.68 | 43.43 |
| *λ*(Mo Kα), Å | 0.71073 | 0.71073 | 0.71073 |
| $R_F$, $R_{wF}$,[a] % | 4.05, 2.73 ($F > 2.0\sigma(F)$) | 3.96, 6.58 ($I > 2.0\sigma(I)$) | 3.64, 3.10 ($F > 2.0\sigma(F)$) |

[a] $R = \sum||F_o| - |F_c||/\sum|F_o|$; $R_{wF} = \sum w(|F_o| - |F_c|)^2/\sum wF_o^2]$, $w^{-1} = \sigma^2(F) + gF^2$.

**Table 2.** Selected Bond Lengths (Å) and Angles (deg) for Compounds **2**, $(Et_3P)_2Pd(PBN^iPr_2)_2$, **3**, $(Et_3P)_2Pd(PBtmp)_2$, and **4**, $(Et_3P)_2Pt(PBN^iPr_2)_2$

| | **2** | **3** | **4** |
|---|---|---|---|
| B−P | B−P(1) 1.921(5)<br>B′−P(1) 1.921(7) | B(1)−P(1) 1.916(8)<br>B(1)−P(2) 1.932(7)<br>B(2)−P(1) 1.953(7)<br>B(2)−P(2) 1.919(8) | B−P(1) 1.914(7)<br>B′−P(1) 1.934(9) |
| P−M | P(1)−Pd 2.420(2)<br>P(2)−Pd 2.330(2) | P(1)−Pd 2.394(2)<br>P(2)−Pd 2.399(2)<br>P(3)−Pd 2.330(2)<br>P(4)−Pd 2.342(2) | P(1)−Pt 2.426(2)<br>P(2)−Pt 2.288(2) |
| B−N | 1.406(8) | B(1)−N(1) 1.427(8)<br>B(2)−N(2) 1.416(8) | 1.427(11) |
| B−P−B | 75.3(3) | B(1)−P(1)−B(2) 77.5(3)<br>B(1)−P(2)−B(2) 77.9(3) | 73.9(4) |
| P−M−P | P(1)−Pd−P(1′) 74.0(1)<br>P(2)−Pd−P(2′) 107.6(1)<br>P(1)−Pd−P(2) 89.3(1) | P(1)−Pd−P(2) 72.7(1)<br>P(3)−Pd−P(4) 108.2(1)<br>P(1)−Pd−P(3) 161.2(1) | P(1)−Pt−P(1′) 74.7(1)<br>P(2)−Pt−P(2′) 107.4(1)<br>P(1)−Pt−P(2) 89.1(1) |
| P−B−P | 98.5(3) | P(1)−B(1)−P(2) 95.1(4)<br>P(1)−B(2)−P(2) 94.4(3) | 99.7(4) |
| B−P−M | B−P(1)−Pd 74.2(2)<br>B′−P(1)−Pd 74.2(2) | B(1)−P(1)−Pd 76.5(2)<br>B(2)−P(1)−Pd 76.8(2)<br>B(1)−P(2)−Pd 76.0(2)<br>B(2)−P(2)−Pd 77.3(2) | B−P(1)−Pt 74.0(3)<br>B−P(1)−Pt 73.6(3) |

intermediate species **11** are neither isolated nor detected spectroscopically, and it is concluded that the intramolecular dehydrohalogenation of **11** is quite facile. Compounds **1**−**6** are isolated in moderate to low yield as air- and moisture-sensitive crystalline solids. Unlike their main group analogs, none display a normal melting point but instead decompose in a temperature range of 90−200 °C under a nitrogen atmosphere. In fact, **6** also decomposes in solution after several days at room temperature which is similar to the behavior noted in the recently reported studies of this molecule.[2] The $^{31}$P NMR analyses of crude, filtered reaction mixtures indicate that compound **1** is formed in high yield (∼90%), along with a small amount (∼10%) of $(tmpBPH)_2$, but **1** is isolated in only 46% yield due to its very high solubility in the organic solvents used for recrystallization. Compound **3** is formed in about 85% yield, along with about 15% unidentified impurities which provide several $^{31}$P resonances in the range 9.3 −13.9 ppm. This compound is isolated in 30% yield following recrystallization. The $^{31}$P NMR spectra of reaction mixtures containing **2** and **4** also indicate formation of a number of products. Compounds **2** and **4** are produced in ∼15% yield and isolated in 13% and 8% yields, respectively. The only other product identified in these mixtures is the cage species $(^iPr_2NB)_3P_2$.[3] In an effort to improve the yields by removal of the HCl formed in the dehydrohalogenation step, a base, $NEt_3$, was combined with the other reactants; however, no significant improvement was noted. Apparently, competing oxidative addition reactions are operat-

**Scheme 2**

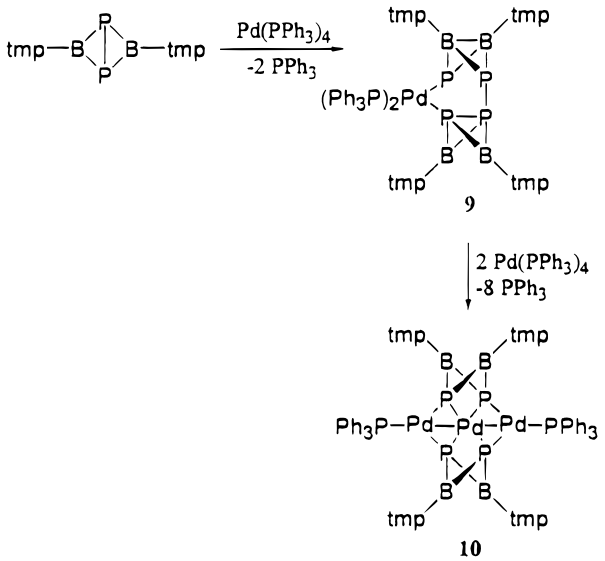

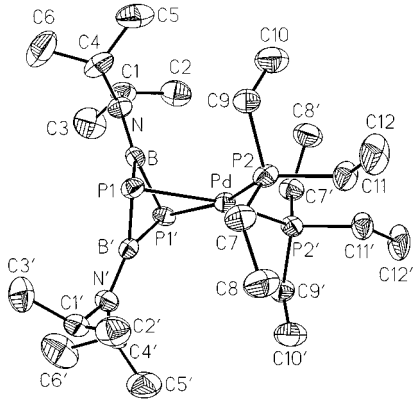


**Figure 1.** Molecular structure and atom-labeling scheme for $P_2(^iPr_2NB)_2Pd(PEt_3)_2$ (**2**).

**Scheme 3**

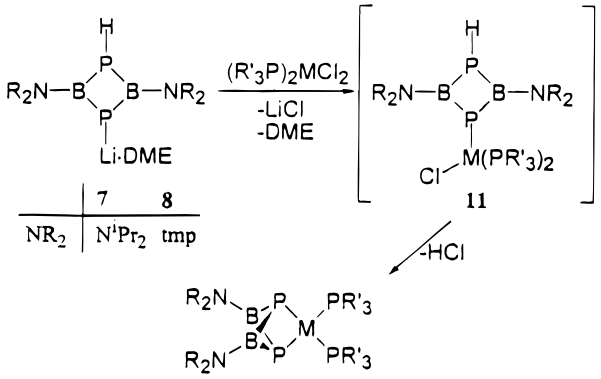


| | 7 | 8 |
|---|---|---|
| $NR_2$ | $N^iPr_2$ | tmp |

| | 1 | 2 | 3 |
|---|---|---|---|
| $NR_2$ | tmp | $N^iPr_2$ | tmp |
| $M(PR'_3)_2$ | $Ni(PEt_3)_2$ | $Pd(PEt_3)_2$ | $Pd(PEt_3)_2$ |
| | **4** | **5** | **6** |
| $NR_2$ | $N^iPr_2$ | $N^iPr_2$ | tmp |
| $M(PR'_3)_2$ | $Pt(PEt_3)_2$ | $Pt(PPh_3)_2$ | $Pt(PPh_3)_2$ |

ing, which produce as yet unidentified products. All cage compounds were finally isolated in spectroscopically pure form except compound **3**, which was typically contaminated with ~5% impurities.

The molecular structures of compounds **2**−**4** were determined by single-crystal X-ray diffraction techniques, and views of the molecules are shown in Figures 1−3. Each can be considered to adopt a trigonal bipyramidal structure with phosphorus atoms occupying the two apical positions and trigonal planar boron atoms as well as a square planar M atom residing on the basal positions. As required by the narrow bite angle of the formal diphosphide ligand fragments $(R_2NBP^-)_2$, the chemically equivalent P atoms reside in *cis* positions on the M atom. Molecules **2** and **4** possess a 2-fold rotation axis that passes through the Pd/Pt atom and the centroid of the folded $B_2P_2$ ring. The general structural features of the compounds, $(R_3P)_2M(PBNR_2)_2$, are similar to the platino compound **6**[2] and the main group analogs, $R_2E(PBNR_2)_2$,[2−8] $R_2E = R_2Si$, $R_2Ge$, and $R_2Sn$, except that the M atoms are in square planar environments rather than tetrahedral.

The structural parameters for **2**, $(Et_3P)_2Pd(PBN^iPr_2)_2$, and **4**, $(Et_3P)_2Pt(PBN^iPr_2)_2$, are almost identical, consistent with the facts that Pd and Pt atoms are similar in atomic size and electronic stuctures.[14] On the other hand, selected structural parameters for **3**, $(Et_3P)_2Pd(PBtmp)_2$, deviate slightly from those

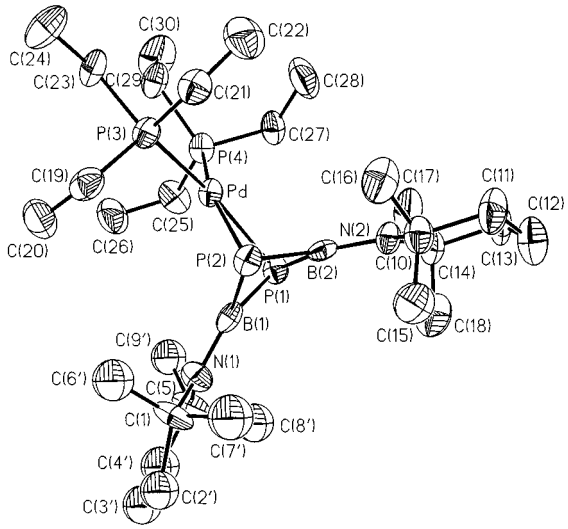


**Figure 2.** Molecular structure and atom-labeling scheme for $P_2(tmpB)_2Pd(PEt_3)_2$ (**3**).

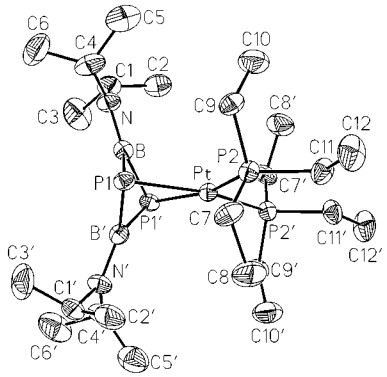


**Figure 3.** Molecular structure and atom-labeling scheme for $P_2(^iPr_2NB)_2Pt(PEt_3)_2$ (**4**).

found in **2**, due to the presence of the larger tmp groups. In each of the molecules, the internal angles at the apical phosphorus atoms are acute: B−P−B; **2**, 75.3(3)°; **3,** 77.7° (average); **4**, 73.9(4)°. B−P−M: **2**, 74.2°; **3**, 76.7° (average); **4**, 73.8° (average). These data are comparable with values found in **6** and the related main group analogs. As a consequence of the constraints imposed by the geometry of the slightly folded $P_2B_2$ ring and the relatively large Pt and Pd radii (Pt(II), $r$ = 0.74 Å; Pd(II), $r$ = 0.78 Å),[14] the $P_{cage}-M-P_{cage}$ angles are also very acute (**2**, 74.0(1)°; **3**, 72.7(1)°; **4**, 74.7(1)°), compared to the external $P_{phosphane}-M-P_{phosphane}$ angles: **2**, 107.6(1)°; **3**, 108.2(1)°; **4**, 107.4(1)°. The internal angles at the Pt atom in **6** are comparable: $P_{cage}-Pt-P_{cage}$ 73.3(1)° and $P_{phosphane}-Pt-P_{phosphane}$ 101.8(1)°. The $P_{cage}-Sn-P_{cage}$ angles found in $[(Me_3Si)_2CH]_2Sn(PBtmp)_2$, 73.8(1)°,[2] $^tBu_2Sn(PBN^iPr_2)_2$, 75.4(1)°,[6] and $^tBu_2Sn(PBtmp)_2$, 73.1(1)°,[6] also are similar due to the comparable size of the Sn(IV) atom (Sn(IV), $r$ = 0.69 Å).[14] However, the corresponding $P_{cage}-Ge-P_{cage}$ angle in $Ph_2Ge(PBtmp)_2$, 80.7(1)°[5] (Ge(IV), $r$ = 0.53Å),[14] and the $P_{cage}-Si-P_{cage}$ angles in $Ph_2Si(PBN^iPr_2)_2$, 85.7(1)°,[4] and $Ph_2Si(PBtmp)_2$, 84.8(1)°[4] (Si(IV), $r$ = 0.40 Å),[14] are larger due to the smaller radii of Ge and Si. The B−P bond lengths for **2**−**4** fall in the single bond range for $sp^2$-hybridized boron atoms:[1] **2**, 1.921 Å (average); **3**, 1.930 Å (average), **4**, 1.924 Å (average). The $P_{cage}-Pd/Pt$ bond lengths are relatively long (**2**, 2.420(2) Å; **3**,

(14) Huheey, J. E. *Inorganic Chemistry: Principles of Structure and Reactivity*, 3rd Ed.; Harper & Row Publishers: New York, 1983.

2.397 Å (average); **4**, 2.426(2) Å), while the $P_{phosphane}$−Pd/Pt bond lengths (**2**, 2.330(2) Å; **3**, 2.336 Å (average); **4**, 2.288(2) Å), are in the normal range for phosphane Pd(II)/Pt(II) complexes.[15] The same trend was found in **9**: $P_{cage}$−Pt, 2.413-(2) Å; $P_{phosphane}$−Pt, 2.320(2) Å.[2] The long $P_{cage}$−Pd/Pt bond lengths together with the small values for the corresponding bond angles around the $P_{cage}$ and Pd or Pt atoms suggest that there is only a small amount of s character in the orbitals that form the $P_{cage}$−Pd/Pt bonds.

The cage compounds **1**−**6** were further characterized by infrared, FAB-MS, and NMR spectroscopic techniques, and these data are consistent with the composition and trigonal bipyramidal structures deduced from the crystallographic analyses of **2**−**4**. The data recorded here for **6** are identical to those reported earlier.[2] The compounds show parent ions in high-resolution FAB-MS analysis, and the parent ion masses match satisfactorily with the theoretical molecular weights of the compounds. The $^{31}$P NMR spectra for **1**−**5** display AA′XX′ patterns with the chemical shifts in the range $\delta$ 14.0 to −68.1 ppm. In each case, the upfield resonance is broader than the downfield resonance and is assigned to the apical, three-coordinate phosphorus atoms in the cage unit. The sharper downfield resonance is assigned to the terminal $R_3P$ ligands. Specifically, the $^{31}$P NMR shifts for the new $B_2P_2Pt$ cage compounds are $\delta$ 12.1 and −68.1 for **4** and $\delta$ 24.9 and −49.5 for **5**. These data are similar for **6**: $\delta$ 21.1 and −5.1. The chemical shifts for the phosphane ligands in **4**−**6** are shifted slightly to lower field relative to the respective precursor compounds: *cis*-$(Et_3P)_2PtCl_2$,[16] $\delta$ 9.0, and *cis*-$(Ph_3P)_2PtCl_2$, $\delta$ 15.7.[17] The $^{31}$P chemical shifts for the $P_{cage}$ atoms are upfield relative to the shifts for the related main group element cages, $R_2E(PBNR_2)_2$, suggesting that the $(R_3P)_2Pt$ groups are more electron releasing than the main group element fragments, $R_2E$. In addition, replacement of the $N^iPr_2$ group with tmp in otherwise identical compounds, e.g., **5** vs **6**, results in a significant downfield shift for the P cage resonance, and a similar trend has been observed with cages containing main group fragments $R_2E$.

The full extent of the possible AA′XX coupling in **4** and **5** is not resolved. One-bond P−Pt coupling involving the *exo* phosphane ligands, $PR_3$, is observed: **4**, 3121 Hz; **5**, 3235 Hz. These values are similar to that in **6**, 3132 Hz, and slightly smaller than the data reported for *cis*-$(Et_3P)_2PtCl_2$,[16] 3502 Hz, and *cis*-$(Ph_3P)_2PtCl_2$,[17] 3608 Hz. The one bond $P_{cage}$−Pt coupling is not resolved for the apical P atom resonance in **4** and **5**, consistent with the structural data, which suggest that there is only a small amount of s character in the orbitals that form the $P_{cage}$−Pt bonds. Both A and X $^{31}$P NMR resonances for **4** are further split into doublets, $J$ = 18 Hz, which most likely result from *trans*-two-bond P−Pt−P′ coupling. The small value of these coupling constants is consistent with the [$R_2$-NBP] fragment acting as a phosphido ligand.[18] The *cis*-two-bond P−Pt−P′ coupling is not resolved. The assignment of the doublet splitting to *trans*-two-bond P−Pt−P′ coupling is based upon the common observation that *trans*-two-bond P−Pt−P′ coupling is greater than *cis*-two-bond P−Pt−P′ coupling in most phosphane Pt complexes.[18] In contrast, the low-field resonance for the $PPh_3$ groups in **5** is split into a pseudotriplet due to two bond coupling from both *cis*- and *trans*-$P_{cage}$ atoms $(|^2J(P,P')_{cis} + {}^2J(P,P')_{trans}|) = 22$ Hz. No splitting is resolved in the upfield resonance. For comparison, **9** shows pseudotriplet patterns for both upfield and downfield resonances with $|^2J(P,P')_{cis} + {}^2J(P,P')_{trans}| = 12$ Hz.

The $^{31}$P NMR spectra for compounds **1**−**3** also show two resonances. Once again, the upfield, relatively broad resonance is assigned to the apical phosphorus atoms and the downfield resonance is assigned to the terminal phosphane ligands. The resonance for the $PEt_3$ groups in **1**, $\delta$ 14.0, is slightly downfield relative to the resonance for $(Et_3P)_2NiCl_2$,[17] $\delta$ 7.1. The resonances for the $PEt_3$ groups in both **2**, $\delta$ 12.2, and **3**, $\delta$ 9.3, are upfield relative to the resonance for $(Et_3P)_2PdCl_2$,[19] $\delta$ 17.8. Similarly, the $^{31}$P NMR chemical shifts of the cage P atoms are upfield relative to those found for the corresponding main group element cage analogs. The resonances for compounds **1** and **3** are split into irregular multiplets arising from partially resolved two bond couplings in the AA′XX′ spin systems. The $(|^2J(P,P')_{cis} + {}^2J(P,P')_{trans}|)$ values are estimated as 14 Hz for **1** and 12 Hz for **3**. The P−P′ splitting is not resolved for compound **2**. $^1$H and $^{13}$C{$^1$H} spectra were also recorded for compounds **1**−**5**, and the data are consistent with the structures of the compounds described above.

Last, it is important to note some mechanistic aspects of the cage formation chemistry shown in Scheme 3. *cis*-$(Ph_3P)_2PtCl_2$ and *cis*-$(Et_3P)_2PtCl_2$ were used in the reactions to produce cage compounds **4** and **5**, and the *cis*-conformation is retained on the Pt fragment. However, there are apparent *trans*- to *cis*-transformations on the Ni and Pd fragments since *trans*-$(Et_3P)_2PdCl_2$ and *trans*- $(Et_3P)_2NiCl_2$ were used in the reactions. Of course, a *cis*-conformation is required by the chelating diphosphide nature of the $[R_2NP^-]_2$ fragment and the barriers to *cis*−*trans* interconversion for the square planar precursors are low.[20] It is interesting that no evidence has been found for the diphosphide fragment acting as a bridging ligand between two metal centers. Further, the reactions may be depicted as nucleophilic substitutions by the phosphide anions $(R_2N)\overline{BP(H)B(NR_2)PLi}\cdot DME$ on the $(R_3P)_2MCl_2$ fragments. The substitutions generate intermediates $(R_2N)\overline{BP(H)B(NR_2)P}M(Cl)(PR_3)_2$ (**11**) that undergo rapid intramolecular HCl eliminations producing the cage compounds $(R_3P)_2M(PBNR_2)_2$. Spontaneous HCl elimination is not observed in most main group element cage formation reactions. Instead, stable intermediates, $(R_2N)\overline{BP(H)B(NR_2)PE(Cl)}R_n$, are normally isolated and cage closure usually requires assistance by addition of a base.

**Conclusion.** The systematic synthetic approach for $B_2P_2E$ cage compound assembly that utilizes small boron−phosphorus ring compounds as building blocks and addition and elimination reactions with other moieties to develop cage structures has been extended here to include species containing boron, phosphorus, and transition metal (nickel, palladium, or platinum) atoms. Unfortunately, at this stage, the yields of the isolated Pd and Pt compounds remain low due to a combination of high solubility and available competing reactivity that produces other products. Still, this approach allows for the formation of several cage

(15) Wilkinson, G.; Stone, F. G. A.; Abel, E. W. *Comprehensive Organometallic Chemistry*; Pergamon Press: London, 1983; Vol. 6, Chapter 39.
(16) Favey, R.; Roulet, R.; Pinkerton, A. A.; Schwarzenbach, D. *Inorg. Chem.* **1980**, *19*, 1356.
(17) Samples were made by dissolving commercial *cis*-$(PPh_3)_2PtCl_2$ in $CH_2Cl_2$ and $(PEt_3)_2NiCl_2$ in $C_6D_6$, and the spectra were recorded on a Bruker WP-250 spectrometer.
(18) (a) Verkade, J. G.; Quin, L. D. *Phosphorus-31 NMR Spectroscopy in Stereochemical Analysis*; VCH Publishers, Inc.: Weinheim, Germany, 1987; Chapter 16. (b) Chatt, J.; Hitchcock, P. B.; Pidcock, A.; Warrens, C. P.; Dixon, K. R. *J. Chem. Soc., Dalton Trans.* **1984**, 2237.
(19) Mann, B. E.; Shaw, B. L.; Slade, R. M. *J. Chem. Soc. A* **1971**, 2976.
(20) Redfield, D. A.; Cary, L. W.; Nelson, J. H. *Inorg. Chem.* **1975**, *14*, 50.

compounds that could not be obtained by the use of low-valent metal fragment addition across the P−P bond in the $[(tmp)BP]_2$ bicycle. The latter route is, of course, also currently limited by the lack of other readily available $[R_2NBP]_2$ bicycles. The successful synthesis of new cage species containing metals suggests that a number of other $B_XP_YM$ cage compounds should be accessible through related chemistry.

**Acknowledgment** is made to the National Science Foundation (Grant CHE-9508668) for support of this research. The cooperation of the University of Nebraska Midwest Center for Mass Spectrometry, where FAB-MS data were obtained, is also noted.

**Supporting Information Available:** X-ray crystallographic files, in CIF format, are available the Internet only. Access information is given on any current masthead page.

IC970965S